Materials Research Express

PAPER

Tribological and mechanical properties of copper matrix composites reinforced with carbon nanotube and alumina nanoparticles

To cite this article: Yu Pan *et al* 2019 *Mater. Res. Express* **6** 116524

Materials Research Express

PAPER

RECEIVED
4 June 2019

REVISED
30 August 2019

ACCEPTED FOR PUBLICATION
20 September 2019

PUBLISHED
2 October 2019

Tribological and mechanical properties of copper matrix composites reinforced with carbon nanotube and alumina nanoparticles

Yu Pan[1], Xin Lu[1], Alex A Volinsky[2], BoWen Liu[1], ShiQi Xiao[1], Chuan Zhou[1], Yang Li[3], MingYin Chen[1] and XuanHui Qu[1]

[1] Beijing Advanced Innovation Center for Materials Genome Engineering, Institute for Advanced Materials and Technology, University of Science and Technology Beijing, Beijing 100083, People's Republic of China

[2] Department of Mechanical Engineering, University of South Florida, Tampa, FL 33620, United States of America

[3] Department of Chemical Engineering, Polytechnique Montreal, Montreal, Quebec H3C 3A7, Canada

E-mail: luxin@ustb.edu.cn

Keywords: copper matrix composites, carbon nanotube, alumina, friction, wear

Abstract

Copper is widely used as electrical contact materials due to its excellent thermal and electrical conductivity. However, low strength and poor wear resistance restrict its practical applications. Herein, we report a high-performance copper matrix composite reinforced with carbon nanotubes (CNT) and alumina (Al_2O_3) nanoparticles prepared by powder metallurgy route. The microstructure, density, hardness, tensile strength and tribological properties were studied. CNTs and Al_2O_3 were successfully mixed with copper powders by acid treatment and mechanical milling. After sintering, CNTs and Al_2O_3 were uniformly distributed around the grain boundaries and limited the grain growth. Furthermore, all copper matrix composites showed decreased density, but increased hardness and tensile strength compared with the copper matrix. More importantly, the incorporation of CNTs and Al_2O_3 significantly improved the tribological properties of copper matrix. This is because Al_2O_3 nanoparticles with high strength enhanced the wear resistance by dispersion strengthening, while CNTs served as solid lubricant greatly improving the anti-friction properties. Besides, the friction coefficient as well as wear rate increased with higher load and sliding speed. The Cu-1.5CNTs-0.5Al_2O_3 composite had the optimal hardness, tensile strength, anti-friction, and wear-resistance properties.

1. Introduction

Copper has been extensively used because of its high heat and electrical conductivity [1–3]. However, copper alloys have low strength and hardness, along with poor tribological properties, which limit their practical applications. They can be damaged by heavy loads or high sliding speeds in friction and wear processes [4–6]. Thus, the research and development of high-performance copper matrix composites are particularly important.

Nowadays, many researchers have tried to enhance the mechanical and tribological properties of copper matrix by adding secondary and/or tertiary phase particles. Ramesh *et al* investigated the mechanical properties and wear resistance of Cu-TiO_2-boric acid hybrid composites. Results show that the composites have superior microhardness, tensile strength and lower wear rate compared with the copper matrix [7]. Chen *et al* fabricated copper matrix composites reinforced with copper-coated $NbSe_2$ and/or carbon nanotubes (CNTs) via a powder metallurgy route, and found that they exhibited high mechanical strength and improved wear resistance [8]. Sharma *et al* reported the fretting wear of copper-TiB_2 and/or Pb composites. The hard TiB_2 reinforcement enhanced the hardness and soft Pb phase served as a solid lubricant, significantly improving the wear-resistance [9]. Additionally, Fathy *et al* improved the compressive and tribological properties of copper matrix with the nano-sized Al_2O_3 addition, and explored the Al_2O_3 dispersion strengthening effects on hardness, compression strength and wear resistance [10].

Alumina is potentially attractive as reinforcement for copper matrix composites due to its good properties, such as high hardness, high strength, excellent thermodynamic stability and abundant resource [11–13].

However, the copper matrix composites strengthened by Al_2O_3 nanoparticles are generally prepared by the internal oxidation method, which is complex and easily results in a non-homogeneous distribution of oxide particles [12, 14]. Thus, Chandrasekhar *et al* prepared Cu–Al_2O_3 composites by combining mechanical alloying and spark plasma sintering, resulting in a homogeneous distribution of Al_2O_3 particles, and three-fold enhanced hardness and strength compared with the copper matrix [13, 15]. Although the mechanical properties were greatly enhanced, the tribological improvements of Cu–Al_2O_3 composites were limited because the hard phase can be easily dropped from the matrix and clogged between the surfaces during rubbing [7, 16]. In this case, carbon nanotubes have superior self-lubricating properties and can effectively improve the wear resistance of composites due to they contain graphite. It is an outstanding reinforcement for developing high wear-resistant copper matrix composites [17–21]. Huang *et al* measured the tribological properties of Cu-CNTs composites, which obviously increased with the incorporation of CNTs. They considered that the excellent friction-reducing and anti-wear properties, as well as the load-carrying capacity of CNTs, offer a good protection of the composites [22]. Therefore, CNTs are good candidates to further improve the tribological properties of copper matrix composites. However, there are not so many researches on the CNTs and Al_2O_3-reinforced copper matrix composites mechanical and tribological properties.

Therefore, this work choses Al_2O_3 nanoparticles as strengthening phase and CNTs as solid lubricant, in order to improve the mechanical and tribological properties of copper matrix composites. The microstructure, density, hardness, tensile strength and tribological properties of the composites reinforced with CNTs and/or Al_2O_3 were investigated. This work provides an effective strategy to fabricate high-property copper matrix wear-resistance composites.

2. Experimental details

2.1. Materials

Cu powders (99.8% purity, an average particle size of 20 μm) and Al_2O_3 nanoparticles (99.5% purity, particle size range of 20–100 nm) provided by the Beijing Xing Rong Yuan Technology Co., Ltd were used as raw materials. Furthermore, the multi-wall CNTs (98% purity, 30–50 nm diameter and 5–10 μm long) prepared by chemical vapor deposition (CVD) process were supplied by the Carbon Nano-material Technology Co., Ltd

2.2. Composite fabrication

The fabrication steps of Cu/CNTs/Al_2O_3 composites are the same as our previous report [19]. Firstly, the original CNTs were pretreated by the mixture of H_2SO_4/HNO_3 solution (volume ratio of 3:1) to prepare the purified CNTs. Secondly, the Cu/CNTs composite powders were prepared by mixing of the obtained CNTs, $Cu(CH_3COO)_2{\cdot}H_2O$ and NaOH in deionized water, and then conducting reduction reaction at 280 °C for 2 h under H_2 atmosphere. Thirdly, the Cu/Al_2O_3 composite powders were fabricated by the high-energy vibrational mixing of Cu and Al_2O_3 powders, in which the anhydrous ethanol act as milling medium. Fourthly, the preapared Cu/CNTs and Cu/Al_2O_3 composite powders were mixed into the Cu/CNTs/Al_2O_3 composite powders by low-energy planetary mill. Three kinds of composite powders were obtained (Cu-0.5Al_2O_3, Cu-1.5CNTs, and Cu-1.5CNTs-0.5Al_2O_3, all in mass ratios). Finally, the as-prepared composite powders were sintered by SPS process at 850 °C for 5 min. Furthermore, the pure Cu powders were sintered by the same way to fabricate a contrast sample. Cylindrical sintered samples were obtained with 30 mm in diameter and 5 mm in height.

2.3. Microstructure and mechanical properties characterization

The microstructure of the powders and as-sintered composites was characterized by field emission scanning electron microscope (FESEM, Quanta FEG 450, USA). The crystallinity and structural integrity of multi-wall CNTs were characterized by Raman spectroscopy (Renishaw inVia, UK). The experimental density of the copper and its composites was tested by Archimedes method. The Cu/CNTs interface structure was characterized by transmission electron microscopy (TEM, H-800, Japan). Vickers hardness were determined by microhardness tester (WOLPERT 430SVD, China) with a load of 100 g and loading time of 15 s. Tensile tests were carried out using an INSTRON 4206 apparatus under a strain rate of 0.002 s^{-1} at room temperature. Three tests were conducted for each set of sample to guarantee the accuracy of data. After tensile tests, the fracture surfaces of the specimen was observed by FESEM.

2.4. Tribological properties

The tribological properties were characterized by WTM-2E controlled atmosphere friction and wear tester. All experiments were carried out in the air at 55 $\pm$ 5% relative humidity and 20 $\pm$ 2 °C temperature. The cylindrical specimen was sliding against a rotating ZrO_2 ball. The counterpart of ZrO_2 ball is 3 mm in diameter

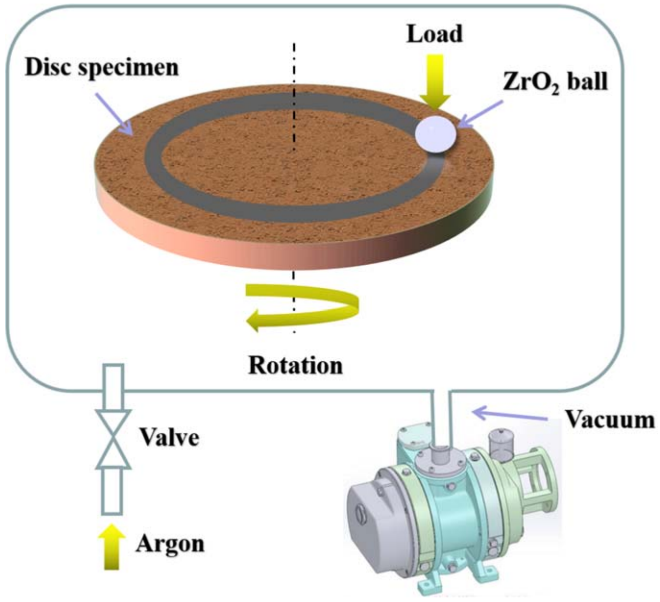

Figure 1. Schematic diagram of the tribological properties test.

and 76 HRC in hardness. Prior to testing, the disc specimen with 15 mm diameter and 5 mm height was polished with a 1000-grit polishing paper, and then cleaned with ethanol in an ultrasonic cleaner. Figure 1 shows the schematic diagram of the tribological tests, which was conducted under dry friction for 10 min, with the sliding speed of 200 rpm (0.063 m s^{-1}), 300 rpm (0.094 m s^{-1}), 400 rpm (0.126 m s^{-1}), and 500 rpm (0.157 m s^{-1}) and load of 2 N, 3 N, 4 N, and 5 N.

After tribological test, the wear loss was weighed by an analytical balance (0.0001 g resolution). The wear rate K was calculated as:

$$K = \frac{V}{P \cdot L} \tag{1}$$

Where V is the wear volume, which is computed from the weight of wear loss, P is load, and L is sliding distance. Three tests were conducted for each set of sample. The worn surfaces and wear tracks were determined by scanning electron microscope (SEM, LEO 1450, Germany). Energy dispersive x-ray spectroscopy (EDS) was used for the wear tracks phase composition analysis.

3. Results and discussion

3.1. Microstructural characteristics

Figure 2 shows the morphology of the raw materials. The images reveal that Cu powders are composed of dendritic particles with a large specific surface area (figure 2(a)) and nano-Al_2O_3 powders are nearly spherical (figure 2(b)). Pristine CNTs prepared by CVD way are seriously tangled together (figure 2(c)), which would increase the difficulty in subsequent homogeneous mixing. However, the CNTs aggregations were significantly improved after acid treatment. Figure 2(d) shows the pretreated multi-wall CNTs are mutually dispersed and their surfaces are relatively smooth.

The Raman spectra of pristine CNTs and CNTs after acid treatment are shown in figure 3. The D-band is associated with the disorder of graphite and G-band is related to the order of crystalline structure. The degree of structural defects as well as disorder in CNTs is usually analyzed via the intensity ratio of I_D/I_G. In comparison with pristine CNTs, the CNTs after acid treatment have slight decrease of ID/IG ratio. This indicates that CNTs have the lessened impurity and also retain the primitive structure after the dispersion process.

Figure 4 exhibits the microstructure characteristics of copper and its composites. The four samples are all compact and have a high density. In addition, there are some granular phases distributed at the grain boundaries for the Cu-0.5Al_2O_3 composite (figure 4(b)) or fibrous phases for the Cu-1.5CNTs composite (figure 4(c)). EDS results indicate that the granular phases are Al_2O_3 and fibrous phases are CNTs. In particular, for the Cu-1.5CNTs-0.5Al_2O_3 composite, these Al_2O_3 nanoparticles and CNTs are distributed uniformly around the grain boundaries, and the grain size is about 4 μm, smaller than pure Cu. Moreover, figure 5 shows the CNTs is

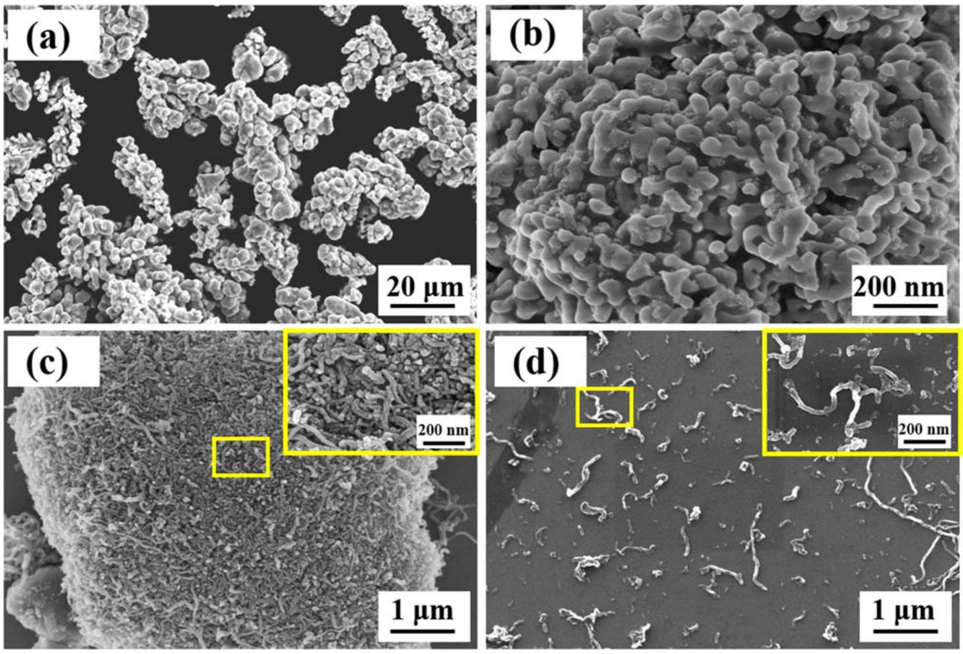

Figure 2. SEM images of (a) pure Cu, (b) nano-Al_2O_3, (c) pristine CNTs, (d) CNTs after acid treatment (Inset in figure 2c and d show the magnified image of the rectangular zone).

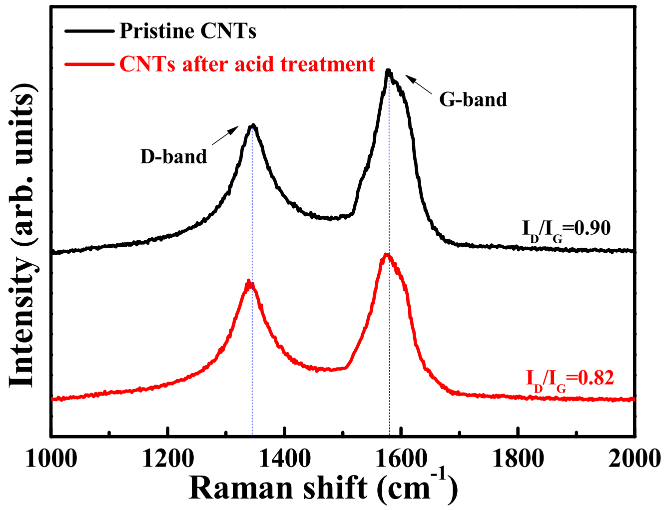

Figure 3. Raman spectra of the pristine CNTs and CNTs after acid treatment.

tightly attached to the copper matrix, and no apparent cracks or pores exist, indicating a strong interfacial adhesion for the Cu-1.5CNTs-0.5Al_2O_3 composite.

3.2. Mechanical properties

Table 1 exhibits the relative density, Vickers hardness and tensile test results of copper and its composites. The relative density of all composites is slightly lower than pure Cu because of the mismatch of thermal expansion coefficient for copper matrix, Al_2O_3, and CNTs [18]. However, every composite keeps a high density of larger than 97%. Additionally, the reinforcement addition effectively strengthens the Vickers hardness of the copper matrix, especially for the Al_2O_3 particles. For the Cu-1.5CNTs-0.5Al_2O_3 composite, the Vickers hardness can reach up to 131 HV, 81.9% higher than pure Cu. Besides, it can be found that the incorporation of CNTs and/or Al_2O_3 greatly increases the tensile strength, while it decreases the elongation of the copper matrix. Among all copper matrix composites, the Cu-1.5CNTs-0.5Al_2O_3 composite owns the highest ultimate tensile strength of 345 MPa.

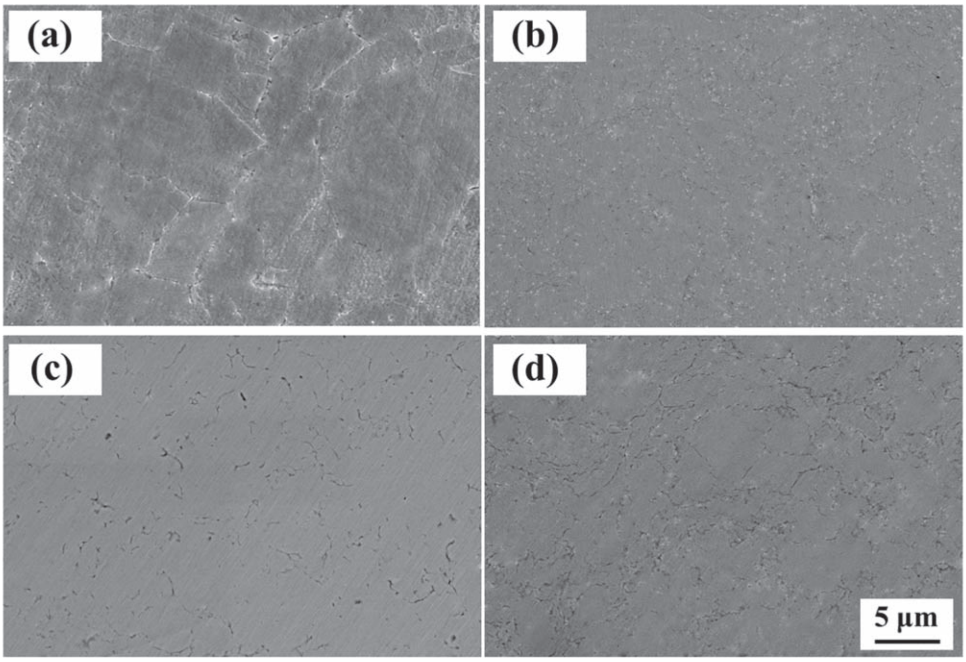

Figure 4. Microstructure of copper and its composites: (a) pure Cu, (b) Cu-0.5Al_2O_3, (c) Cu-1.5CNTs, (d) Cu-1.5CNTs-0.5Al_2O_3.

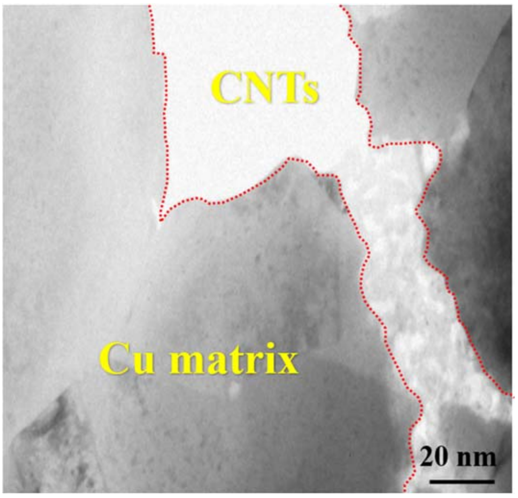

Figure 5. TEM image of Cu/CNTs interface structure for the Cu-1.5CNTs-0.5Al_2O_3 composite.

Table 1. Relative density, Vickers hardness and tensile properties of copper and its composites.

Sample composition, wt%	Relative density, % theoretical density	Vickers hardness, HV	Ultimate tensile strength, MPa	Elongation, %
Cu	99.6 ± 0.3	72 ± 5	199 ± 21	29.6 ± 2.4
Cu-0.5Al_2O_3	98.8 ± 0.2	115 ± 6	292 ± 20	11.5 ± 1.6
Cu-1.5CNTs	99.1 ± 0.4	96 ± 3	244 ± 16	10.1 ± 1.9
Cu-1.5CNTs-0.5Al_2O_3	97.8 ± 0.3	131 ± 5	345 ± 18	13.8 ± 2.1

Figure 6 shows the FESEM images of fracture surfaces of Cu-1.5CNTs-0.5Al_2O_3 composite after tensile testing. It can be seen that many dimples are shown in the fracture surfaces, consistenting with its good plasticity. Moreover, Al_2O_3 particles are evenly dispersed in the bottom of the fracture dimples (figure 6(a)). In the figure 6(b), some short CNTs are found to be pulled out on the fracture surface. This further confirm the strong interface in the Cu-1.5CNTs-0.5Al_2O_3 composite, which can block the propagation of cracks.

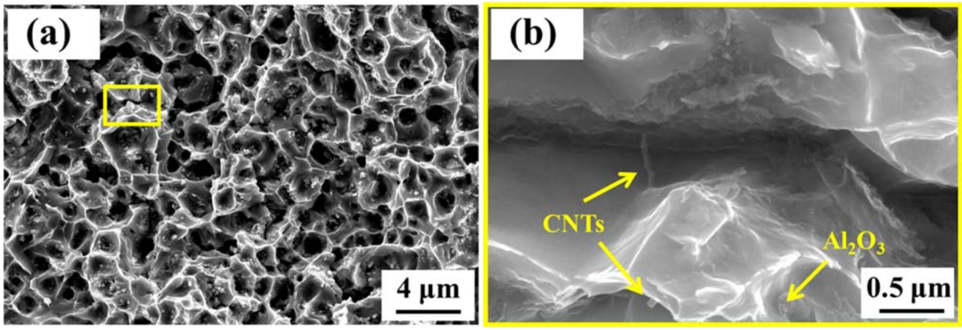

Figure 6. FESEM images of fracture surfaces of the Cu-1.5CNTs-0.5Al_2O_3 after tensile testing.

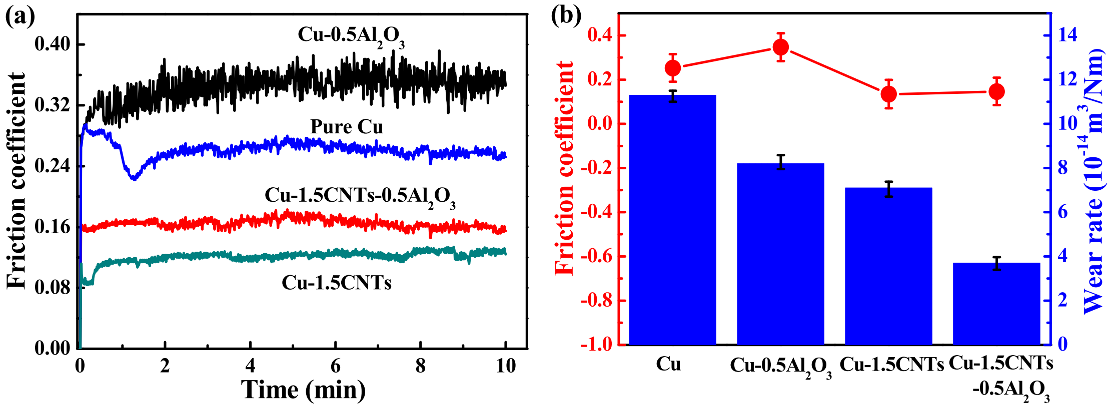

Figure 7. (a) Typical friction coefficient curves and (b) comparisons of corresponding average friction coefficient and wear rate of copper and its composites under constant condition (3 N, 0.094 m s^{-1}, 10 min).

The strengthening mechanism of the Cu-1.5CNTs-0.5Al_2O_3 composite can be summarized to be synergistic effects of the Orowan mechanism of Al_2O_3 and load transfer of CNTs. Due to the high hardness and strength, Al_2O_3 particles are hard to be cut off in the process of dislocation motion. Therefore, the dislocation migration is restricted by the dispersive Al_2O_3 particles and form a effective dispersion strengthening effect. Besides, CNTs have superior mechanical properties and good interfacial bonding. When the composites under high load, the stresses could be transferred to CNTs through interfacial shear stresses originating from the copper matrix. Thus, CNTs could effectively bear a part of load and improve the mechanical properties of the composites.

3.3. Friction and wear properties

Figure 7(a) presents variation of typical friction coefficient curves of copper and its composites under constant condition (3 N, 0.094 m s^{-1}, 10 min). It is clear that the Al_2O_3 addition in the copper matrix leads to an increased friction coefficient. The Cu-0.5Al_2O_3 composite exhibits the highest friction coefficient and has higher volatility. This is due to the fact that harder Al_2O_3 particles can protrude from the softer copper matrix, and then slide on the worn surfaces during rubbing, increasing the friction coefficient of the composites [5]. When adding CNTs, the friction coefficient of the Cu-1.5CNTs-0.5Al_2O_3 composite consequently decreases and keeps at a stable level (~0.155). In addition, the friction coefficient curve of pure Cu initially displays a 'valley' shape and then tends to be steady at about 2.4 min, suggesting the running-in time is 2.4 min. However, the other copper matrix composites show shorter running-in time due to their high hardness and self-lubricating properties. Generally, the main friction and wear occur in the initial stage of test. Thus, due to the faster running-in process, the composites reinforced with CNTs and Al_2O_3 have excellent anti-friction and wear-resistant properties.

The corresponding average friction coefficient and wear rate of copper and its composites are displayed in figure 7(b). The overall friction coefficient of composites varies in the range of 0.134–0.346. By comparison, the incorporation of CNTs decreases the friction coefficient from 0.252 for the pure Cu to 0.134 for the Cu-1.5CNTs composite. Nevertheless, the incorporation of Al_2O_3 slightly increases the friction coefficient. Moreover, it is shown that the wear resistance of the copper matrix is strengthened by the Al_2O_3 and CNTs addition, and the Cu-1.5CNTs-0.5Al_2O_3 composite presents the lowest wear rate of 3.7×10^{-14} m^3 N^{-1}·m^{-1}. According to the

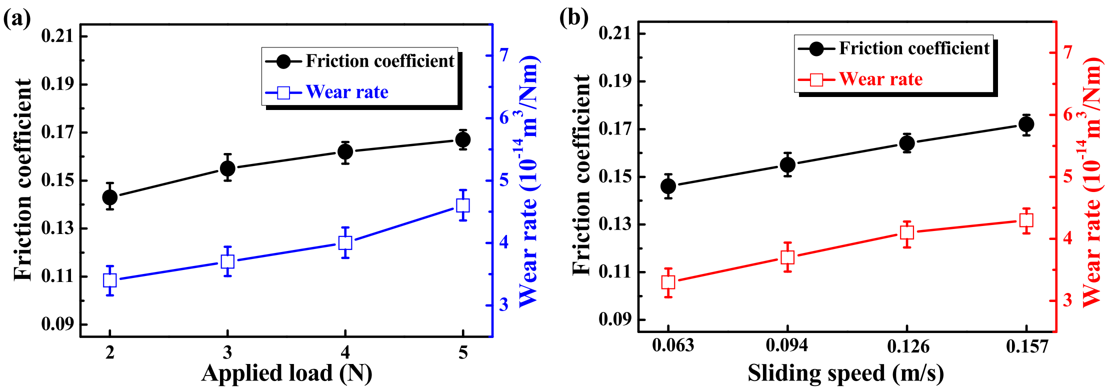

Figure 8. (a) Variation of average friction coefficient and wear rate of the Cu-1.5CNTs-0.5Al_2O_3 composites under different applied loads, (b) under different sliding speeds.

empirical Archards' model [23, 24], the wear resistance of composites is proportional to their hardness. As mentioned above, the incorporation of Al_2O_3 can significantly increase the hardness of composites, and therefore enhancing the wear resistance of the Cu-0.5Al_2O_3 composite. More importantly, the wear rate of the Cu-1.5CNTs-0.5Al_2O_3 composite can further decrease due to the lubricating effect of CNTs. During friction and wear process, the matrix is worn off first, and CNTs are exposed on the worn surface to generate a solid lubricant film. This effectively decreases the contact area between the copper matrix and counterpart, protecting the copper matrix from severe damage. Therefore, the Cu-1.5CNTs-0.5Al_2O_3 composite shows the best tribological properties due to the synergistic effects of Al_2O_3 and CNTs.

As an example of the Cu-1.5CNTs-0.5Al_2O_3 composite, figure 8(a) illustrates variation of the average friction coefficient and wear rate under different applied loads. Obviously, the friction coefficient as well as wear rate increases with load. This is in agreement with some early reports that the metal matrix composites have poor friction and wear performances at high loads [25–29]. During the sliding process, the asperities on the tribosurface of the composites are plastically extruded, fatigue damaged and micro-cut by the counterpart. At higher loads, it is tend to occur larger plastic deformation and increase the depth of asperities penetration, resulting in more serious abrasive wear. Figure 8(b) shows changes of an average friction coefficient and wear rate under different sliding speeds. Similar to figure 8(a), the friction coefficient and wear rate exhibit analogous changes, and increase with sliding speed. It is attributed to the fragmentation of existing solid lubricating film at higher sliding speed. The fragmented solid films could accumulate at the sliding surfaces, leading to a higher friction coefficient. Meanwhile, the high sliding speed would increase the surface friction temperature and expand the contact area between sliding surfaces, causing a severe abrasion and high wear rate.

3.4. Evaluation of worn surfaces

Figure 9 shows the morphology of worn surfaces of copper and its composites after dry friction at a load of 3 N and sliding speed of 0.094 m s^{-1}. It is shown that severe plastic deformation and many plows are found on the worn surface of pure Cu (figures 9(a) and (b)), especially for some large flakes. This indicates that the wear mechanism is adhesive wear and plastic deformation, and is correspond to the above analysis that pure Cu has the highest wear rate. With the incorporation of Al_2O_3, the deep grooves and large plastic deformation are mitigated. The worn surface of the Cu-0.5Al_2O_3 composite is characterized by a relatively smooth surface, while some deep abrasive grooves are also present (figures 9(c) and (d)). Hard Al_2O_3 particles reinforce the copper matrix and impede the severe plastic deformation of the soft copper matrix. Nevertheless, some Al_2O_3 particles may get dislodged from their original microstructure sites during rubbing. Then, they can serve as abrasive particles to abrade the copper matrix surface as well as the counterpart, leaving some deep parallel grooves. Moreover, the tribological properties can be further improved by the incorporation of CNTs. Figures 9(f) and (h) exhibit some lubricating films on the worn surface of the Cu-1.5CNTs composite, but they are exfoliated and intermittent due to the lower hardness of the composite. These lubricating films play an important role in decreasing the friction coefficient and wear rate of the composites under dry friction. On the worn surface shown in figure 9(h), the continuous and uniform lubricating films can largely restrict the plowing effect and preserve the copper matrix from serious abrasion. On the other hand, the lowest wear track width of 198.7 μm also reveals the best wear resistance of the Cu-1.5CNTs-0.5Al_2O_3 composite compared with other composites.

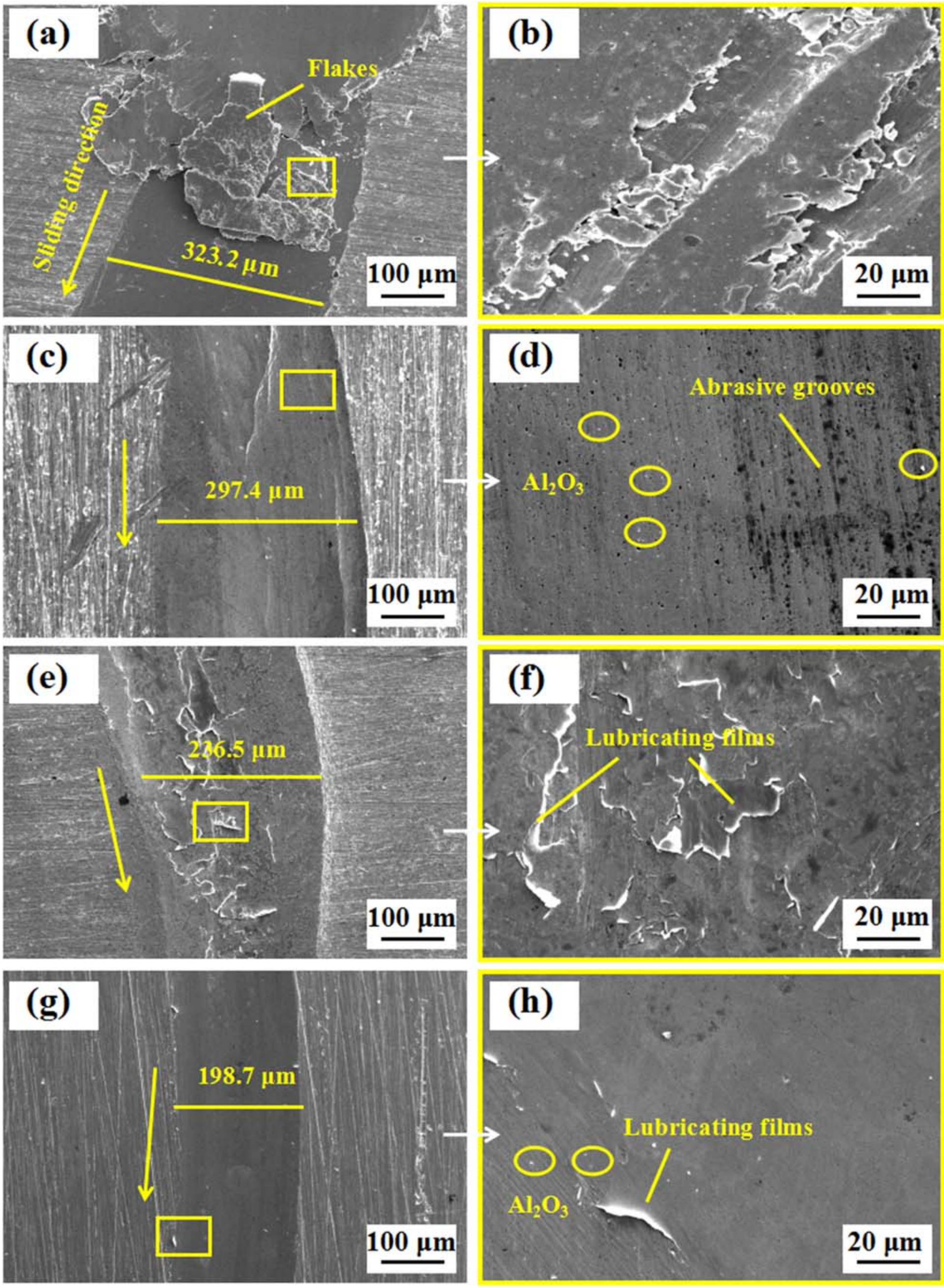

Figure 9. SEM images of worn surfaces of copper and its composites after dry frication at a load of 3 N, sliding speed of 0.094 m s^{-1}: (a) pure Cu, (b) Cu-0.5Al_2O_3, (c) Cu-1.5CNTs, (d) Cu-1.5CNTs-0.5Al_2O_3.

4. Conclusions

Copper matrix composites reinforced with CNTs and Al_2O_3 were successfully synthesized using a powder metallurgy route, and their microstructure, density, mechanical strength and tribological properties were studied. The following conclusions are made:

(1) CNTs and Al_2O_3 are successfully mixed with copper powders by acid treatment and mechanical milling. After sintering, these CNTs and Al_2O_3 distribute uniformly around the grain boundaries and reduce the grain size of the Cu-1.5CNTs-0.5Al_2O_3 composite to 4 μm.

(2) Compared to the copper matrix, copper matrix composites with CNTs and Al_2O_3 have decreased density, but increased hardness and tensile strength.

(3) The tribological properties of the copper matrix are improved significantly with the incorporation of Al_2O_3 and CNTs. The Al_2O_3 with high strength enhance the wear resistance and CNTs serving as solid lubricant

improve the anti-frictional properties. The friction coefficient as well as wear rate increase with the load and sliding speed.

(4) The Cu-1.5CNTs-0.5Al_2O_3 composite displays excellent mechanical and tribological properties, such as 131 HV hardness, 345 MPa tensile strength, 0.155 friction coefficient and 3.7×10^{-14} m^3 N^{-1}·m^{-1} wear rate under constant condition (3 N, 0.094 m s^{-1}, 10 min).

Acknowledgments

This work was supported by the National Natural Science Foundation of China (51874037) and the Weapon Innovation Funds for the '13th Five-Year' (6141B012807).

ORCID iDs

Yu Pan https://orcid.org/0000-0001-5186-144X
Xin Lu https://orcid.org/0000-0002-6711-9888

References

[1] Chu K, Wang X H, Wang F, Li Y B, Huang D J, Liu H, Ma W L, Liu F X and Zhang H 2018 Largely enhanced thermal conductivity of graphene/copper composites with highly aligned graphene network *Carbon* **127** 102–12
[2] Wang H, Zhang Z, Hu Z Y, Song Q and Yin S P 2018 Interface structure and properties of CNTs/Cu composites fabricated by electroless deposition and spark plasma sintering *Mater. Res. Express* **5** 015602
[3] Somani N, Tyagi Y, Kumar P, Srivastava V and Bhowmick H 2019 Enhanced tribological properties of SiC reinforced copper metal matrix composites *Mater. Res. Express* **6** 016549
[4] Cui G J, Bi Q L, Niu M, Yang J and Liu W M 2013 The tribological properties of bronze-SiC-graphite composites under sea water condition *Tribol. Int.* **60** 25–35
[5] Cui G J, Bi Q L, Yang J and Liu W M 2013 Fabrication and study on tribological characteristics of bronze-alumina-silver composite under sea water condition *Mater. Des.* **46** 473–84
[6] Zeng J *et al* 2009 Wear performance of the lead free tin bronze matrix composite reinforced by short carbon fibers *Appl. Surf. Sci.* **255** 6647–51
[7] Ramesh C S, Noor Ahmed R, Mujeebu M A and Abdullah M Z 2009 Fabrication and study on tribological characteristics of cast copper-TiO_2-boric acid hybrid composites *Mater. Des.* **30** 1632–7
[8] Chen B B, Yang J, Zhang Q, Huang H, Li H P, Tang H and Li C S 2015 Tribological properties of copper-based composites with copper coated $NbSe_2$ and CNT *Mater. Des.* **75** 24–31
[9] Sharma A S, Mishra N, Biswas K and Basu B 2013 Fretting wear study of Cu-10 wt% TiB_2 and Cu-10 wt% TiB_2-10 wt% Pb composites *Wear* **306** 138–48
[10] Fathy A, Shehata F, Abdelhameed M and Elmahdy M 2012 Compressive and wear resistance of nanometric alumina reinforced copper matrix composites *Mater. Des.* **36** 100–7
[11] Edalati K, Ashida M, Horita Z, Matsui T and Kato H 2014 Wear resistance and tribological features of pure aluminum and Al–Al_2O_3 composites consolidated by high-pressure torsion *Wear* **310** 83–9
[12] Zhang X H, Li X X, Chen H, Li T B, Su W and Guo S D 2016 Investigation on microstructure and properties of Cu–Al_2O_3 composites fabricated by a novel *in situ* reactive synthesis *Mater. Des.* **92** 58–63
[13] Chandrasekhar S B, Sarma S S, Ramakrishna M, Babu P S, Rao T N and Kashyap B P 2014 Microstructure and properties of hot extruded Cu-1 wt% Al_2O_3 nano-composites synthesized by various techniques *Mater. Sci. Eng. A* **591** 46–53
[14] Ren F Z, Zhi A J, Zhang D W, Tian B H, Volinsky A A and Shen X N 2015 Preparation of Cu–Al_2O_3 bulk nano-composites by combining Cu–Al alloy sheets internal oxidation with hot extrusion *J. Alloys Comp.* **633** 323–8
[15] Chandrasekhar S B, Wasekar N P, Ramakrishna M, Babu P S, Rao T N and Kashyap B P 2016 Dynamic strain ageing in fine grained Cu-1 wt% Al_2O_3 composite processed by two step ball milling and spark plasma sintering *J. Alloys Compd.* **656** 423–30
[16] Ramesh C S, Ahmed R N, Mujeebu M A and Abdullah M Z 2009 Development and performance analysis of novel cast copper-SiC-Gr hybrid composites *Mater. Des.* **30** 1957–65
[17] Xia L, Jia B B, Zeng J and Xu J C 2009 Wear and mechanical properties of carbon fiber reinforced copper alloy composites *Mater. Charact.* **60** 363–9
[18] Wang H, Zhang Z H, Zhang H M, Hua Z Y, Li S L and Cheng X W 2017 Novel synthesizing and characterization of copper matrix composites reinforced with carbon nanotubes *Mater. Sci. Eng. A* **696** 80–9
[19] Pan Y, Xiao S Q, Lu X, Zhou C, Li Y, Liu Z W, Liu B W, Xu W, Jia C C and Qu X H 2019 Fabrication, mechanical properties and electrical conductivity of Al_2O_3 reinforced Cu/CNTs composites *J. Alloys Compd.* **782** 1015–23
[20] Wang Z Q, Ren R R, Song H J and Jia X H 2018 Improved tribological properties of the synthesized copper/carbon nanotube nanocomposites for rapeseed oil-based additives *Appl. Surf. Sci.* **428** 630–9
[21] Faria B, Guarda C, Silvestre N, Lopes J and Galhofo D 2018 Strength and failure mechanisms of cnt-reinforced copper nanocomposite *Compos. B Eng.* **144** 108–20
[22] Huang Z X, Zheng Z, Zhao S, Dong S J, Luo P and Chen L 2017 Copper matrix composites reinforced by aligned carbon nanotubes: mechanical and tribological properties *Mater. Des.* **133** 570–8
[23] Archard J F 1953 Contact and rubbing of flat surfaces *J. Appl. Phys.* **24** 981–8
[24] Cui G J, Bi Q L, Zhu S Y, Yang J and Liu W M 2012 Tribological properties of bronze-graphite composites under sea water condition *Tribol. Int.* **53** 76–86
[25] Pellizzari M and Cipolloni G 2017 Tribological behaviour of Cu based materials produced by mechanical milling/alloying and spark plasma sintering *Wear* **376** 958–67

[26] Liu X Y, Shen Q, Shi X L, Zou J L, Huang Y C, Zhang A, Yan Z, Deng X B and Yang K 2018 Effect of applied load and sliding speed on tribological behavior of TiAl-based self-lubricating composites *J. Mater. Eng. Perform.* **27** 194–201
[27] Mai Y J, Chen F X, Lian W Q, Zhang L Y, Liu C S and Jie X H 2018 Preparation and tribological behavior of copper matrix composites reinforced with nickel nanoparticles anchored graphene nanosheets *J. Alloys Compd.* **756** 1–7
[28] Gyawali G, Tripathi K, Joshi B and Lee S W 2017 Mechanical and tribological properties of Ni-W-TiB_2 composite coatings *J. Alloys Compd.* **721** 757–63
[29] Yang J, Ma J Q, Bi Q L, Liu W M and Xue Q J 2008 Tribological properties of Fe_3Al material under water environment *Mater. Sci. Eng. A* **490** 90–4